Abdominal Radiology (2019) 44:3950–3961
https://doi.org/10.1007/s00261-019-02212-y

SPECIAL SECTION: UROTHELIAL DISEASE

Imaging of the female urethra

Aarti Sekhar[1] · **Linton Eberhardt IV**[1] · **Karen S. Lee**[2]

Published online: 20 September 2019

Abstract
Female urethral pathology can be challenging to diagnose clinically due to non-specific symptoms. High-resolution MRI has become a powerful tool in the diagnosis of urethral lesions and staging of malignancy. Additionally, dynamic MRI, fluoroscopy or ultrasound can evaluate for pelvic floor prolapse and the effectiveness of surgical interventions. This article will review the imaging features of common benign and malignant conditions of the female urethra including diverticula, benign cystic and solid lesions, malignancy, surgical slings, and injection of bulking agents.

Keywords Urethra · MRI · VCUG

Introduction

The female urethra is a short structure that can display a wide range of pathology and non-specific clinical symptoms including dysuria, bleeding, urgency, dribbling and incontinence. Diagnosing the etiology of these symptoms can be challenging, as the cause is often not detectable at physical examination. Historically, voiding cystourethrography (VCUG) and double-balloon catheter urethrography have been utilized for diagnosis. More recently, high-resolution multiplanar magnetic resonance imaging (MRI) has significantly improved our ability to diagnose urethral pathology, while dynamic MRI, fluoroscopy and ultrasound are potent tools for functional imaging of the urethra.

In this article, we will describe normal anatomy of the female urethra and focus on MRI of urethral and periurethral conditions. Topics include benign lesions (diverticula, periurethral cysts, leiomyoma and other solid benign lesions), malignancy (urothelial cancer, squamous cell carcinoma and adenocarcinoma), and post-intervention appearances of the urethra (injection and urethral sling).

Normal anatomy

The female urethra is a relatively short tubular structure, approximately 4 cm in length (compared to 20 cm for the male urethra), embedded in the anterior vaginal wall. This short length predisposes women to urinary tract infections more frequently than men. The urethra begins at the bladder neck and passes through the urogenital diaphragm, opening through the external urethral meatus between the clitoris and the vaginal opening. Many small glands open into the urethra, including two mucous-producing and lubricating Skene glands on either side of the distal urethra.

The urethra consists of three main layers, mucosal, erectile and muscular, which can be delineated on MRI as the normal zonal anatomy of the urethra (Fig. 1). The superficial mucosal layer is continuous proximally with the bladder's transitional epithelium, and distally with the stratified squamous epithelium of the vulva. This geographic variance accounts for urothelial carcinoma affecting the proximal urethra and squamous cell carcinoma affecting the distal urethra. The second layer, the erectile submucosa, contains a rich venous plexus, collagen, and elastic and muscular fibers, helping to keep the urethra closed at rest [1]. The third layer, or "internal urethral sphincter", is composed of smooth muscle with an inner longitudinal layer that shortens

✉ Aarti Sekhar
Aarti.Sekhar@emoryhealthcare.org

Linton Eberhardt IV
leberha@emory.edu

Karen S. Lee
kslee@bidmc.harvard.edu

[1] Department of Radiology and Imaging Sciences, Emory University School of Medicine, 1365 Clifton Rd., Atlanta, GA 30322, USA

[2] Department of Radiology, Beth Israel Deaconess Medical Center, 330 Brookline Avenue, Boston, MA 02215, USA

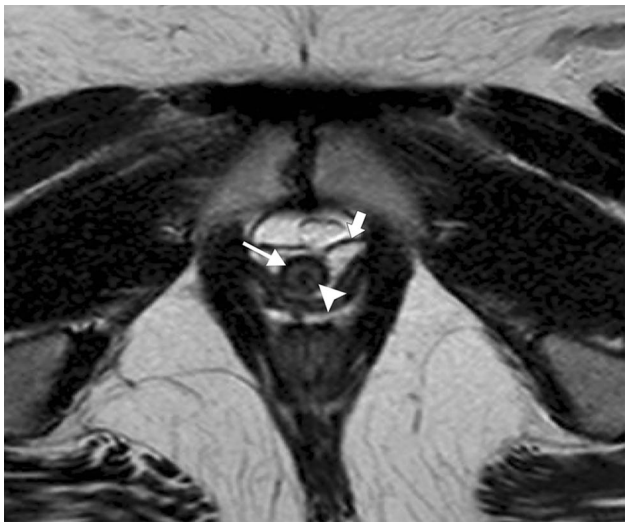

Fig. 1 Normal zonal anatomy of the female urethra on MRI. Axial T2-weighted image demonstrates the target appearance of the normal female urethra. The inner mucosal layer is slightly hypointense on T2WI, the vascularized connective tissue of the submucosa is hyperintense (arrowhead), and the outer muscular layer is hypointense (long arrow). Periurethral ligaments (short arrow) can also be seen

the urethra during micturition and an outer circular layer that provides tone. This smooth muscle layer is controlled by the autonomic nervous system and not under voluntary control. Finally, a complex "external urethral sphincter" composed of skeletal muscle and fibrous tissue surrounds the mid-urethra and can be relaxed during voluntary micturition [1].

The lymphatic drainage of the female urethra also varies based on location within the urethra. The proximal urethra drains into the internal iliac lymph nodes, and the distal urethra drains into inguinal lymph nodes. Nodal drainage is important for staging of malignancy.

Physiologic role of the urethra

At rest, the urethra remains closed because of the fascial/muscular support hammock of the pelvic floor and anterior vaginal wall, the intrinsic tone of the levator ani which keeps the urethrovaginal junction at the bladder neck in an intra-abdominal position, and the resting tone of the striated external sphincter and circular smooth muscle of the internal sphincter [1]. During micturition, the levator ani and sphincters relax, allowing the urethra to descend and funnel into a relaxed open position. This movement can be seen during dynamic imaging. Pelvic floor weakening can lead to stress urinary incontinence and urethral hypermobility, resulting in pelvic floor descent and cystocele development.

Imaging of the urethra: MRI

Due to high spatial resolution, excellent contrast resolution, and superiority in delineating the extent of periurethral disease, MRI has become *the* imaging modality of choice for suspected urethral pathology and pre-operative planning. Common indications for MRI include recurrent urinary tract infections, suspected urethral diverticulum or mass, known colovesical fistula, suspected prolapse, and urinary incontinence [2]. MRI has significantly higher sensitivity and negative predictive values than VCUG [3]. This modality is also ideal for pregnant and pediatric patients given lack of radiation. A dedicated MRI female urethra protocol is recommended to optimize visualization; the imaging protocol used at the authors' institutions is described here.

Coverage

MRI of the female urethra should include coverage of the entire bladder and urethra through the perineum. Patients can be imaged in the supine position at 1.5 or 3T. Use of a pelvic phased array coil provides sufficient coverage of the pelvis. Less commonly, endocavitary (transvaginal or transrectal) coils are used. The patient is asked to empty her bladder 1 h prior to imaging so that the bladder is half full during the exam.

T2wi

High resolution, small field-of-view T2-weighted turbo spin-echo (TSE) sequences in the sagittal, axial and coronal planes provide detailed urethral anatomy. An additional axial TSE with fat saturation (FS) aids in detection of inflammation. T2WI is ideal for evaluating for diverticula and periurethral cysts.

T1wi

Fat-suppressed T1W gradient-recalled echo (GRE) sequences of the pelvis are obtained prior to and following administration of weight-based IV gadolinium contrast agent in the axial plane, with automated subtraction sequences. An additional sagittal post-contrast sequence is obtained. These sequences are critical for tumor assessment. T1W in- and opposed-phase GRE sequences are not routinely necessary, however, can be employed as problem-solving sequences for situations where there may be suspicion for air, metal, or fat.

Diffusion-weighted imaging (DWI)

DWI is optional, but useful for tumor assessment, abscess evaluation, and lymph node detection, and should be performed before gadolinium administration. At least two *b* values, ≤ 100 and > 800, should be obtained to allow calculation of the apparent diffusion coefficient (ADC) map.

Dynamic MRI of the urethra for cystoceles and urethral hypermobility

Dynamic imaging is an optional tool utilized in specific cases of suspected pelvic floor dysfunction; dynamic imaging is not routinely used for suspected malignancy or urethral diverticulum. Imaging is obtained in the sagittal plane using either T2WI or a steady-state free precession sequence, with the patient at rest and maximal strain (Valsalva maneuver) for 5 s intervals. Bennett et al. demonstrated the added utility of dynamic MRI sequences: out of 84 patients with lower urinary tract symptoms, 39.3% of these patients had pelvic floor prolapse *only* diagnosed during strain/dynamic imaging [4].

Imaging of the female urethra: ultrasound

High-resolution transvaginal and transperineal ultrasound are cost-effective imaging techniques utilized in specialized centers. A high-frequency transvaginal probe with 5–9 MHz frequency can be inserted 1–2 cm into the vagina and angled anteriorly to image the entire urethra. Dynamic ultrasound can be performed with the patient straining or voiding to evaluate for urethral mobility and cystocele, as well as sling positioning and function. For transperineal US, a linear-array transducer (5–10 MHz) can be placed on the urethra with a stand-off pad. Sonography is operator dependent and can be limited in distinguishing the origin of cysts and diverticula.

Imaging of the female urethra: fluoroscopy

VCUG offers dynamic evaluation of the female urethra, but has been mostly supplanted by MRI. A transurethral catheter is placed via sterile technique. The bladder is then filled maximally (250–400 cc depending on patient tolerance) with cystographic contrast agent such as Cysto-Conray or Cysto-grafin—these contrast agents have less adverse effects on the bladder. The catheter is removed, and the urethra is imaged fluoroscopically at multiple angles during micturition. Indications for VCUG include evaluation of diverticula, particularly for identification of the neck, and post-repair of urethral diverticula.

Benign lesions: urethral diverticulum

Urethral diverticula (UD) are the most common benign lesions of the female urethra occurring in 6% of women, although this is likely an underestimate as more are being detected incidentally [5]. Diverticula are associated with urethral infection and stress urinary incontinence (SUI). The etiology stems from rupture of dilated or infected periurethral glands. Less frequent etiologies are birth trauma and post-surgical or instrumentation trauma. Noncommunicating diverticula are located within the wall of the urethra and represent the initial stage of diverticulum formation [6].

Symptoms are usually nonspecific such as urinary frequency, infection, and retention. Less commonly, diverticula have a "classic" presentation of the three Ds: dysuria, post-void dribbling (seen in 25% of patients) and dyspareunia (described in 10%). Complications include chronic infection, stone formation (in up to 10%), and malignant degeneration into adenocarcinoma and less likely urothelial or squamous cell carcinoma [7]. Treatment of UD is usually by transvaginal resection of the diverticulum.

MRI is the most sensitive study for detecting and characterizing diverticula and their complications, followed by VCUG, which has an accuracy of 65% [7] and is limited in detection of diverticula that do not communicate with the lumen, termed "non-communicating diverticula". Diverticula are best evaluated on T2WI since most diverticula are fluid-filled (Fig. 2), however, they can be complicated by hemorrhage and stones, both of which may appear hypointense on T2WI (Fig. 3). The diverticula may be uni- or multilocular and are most commonly located along the posterolateral middle third of the urethra. When large, the diverticulum can surround the posterior urethra and produce a "saddle" appearance. An important factor is identifying the neck of the diverticulum if possible, so that the surgeon can resect the neck to prevent recurrence. If the neck cannot be delineated on MRI, fluoroscopy can be complimentary. After diverticulectomy, a VCUG is often performed to evaluate for urethral integrity and diverticulum persistence or recurrence (Fig. 4).

Benign cystic lesions: periurethral cysts

Periurethral cystic lesions include Skene gland cyst, Bartholin gland cyst, and Gartner cyst. These lesions do not communicate with the urethral lumen and are usually asymptomatic and incidental, however, they can present with hemorrhage or pressure from mass effect.

Skene glands, analogous to the male prostate, are paired glands of the external urethral meatus and secrete mucus

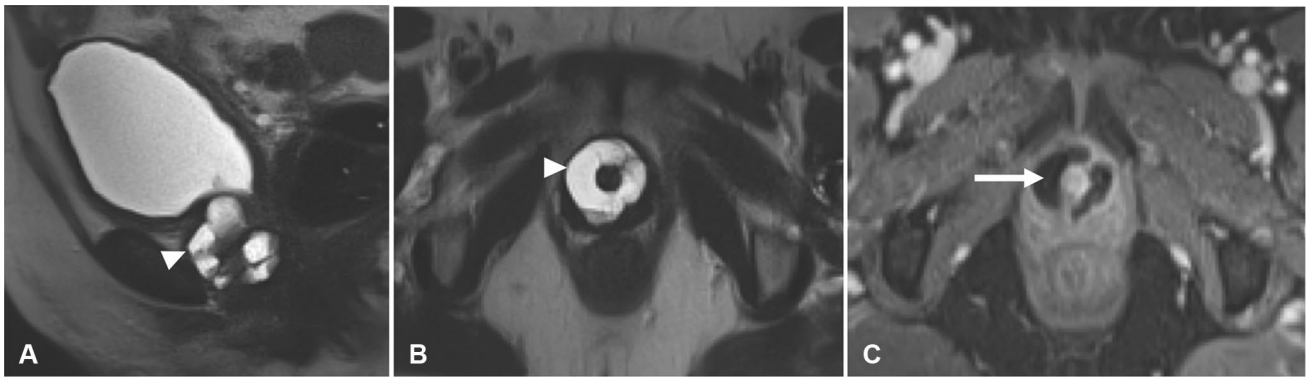

Fig. 2 A "saddle" diverticulum on sagittal (**a**) and axial (**b**) T2WI (arrowheads). This diverticulum wraps around the urethral meatus without a definable neck. On post-contrast T1WI (**c**), there is no nodular internal enhancement (arrow) to indicate malignant degeneration

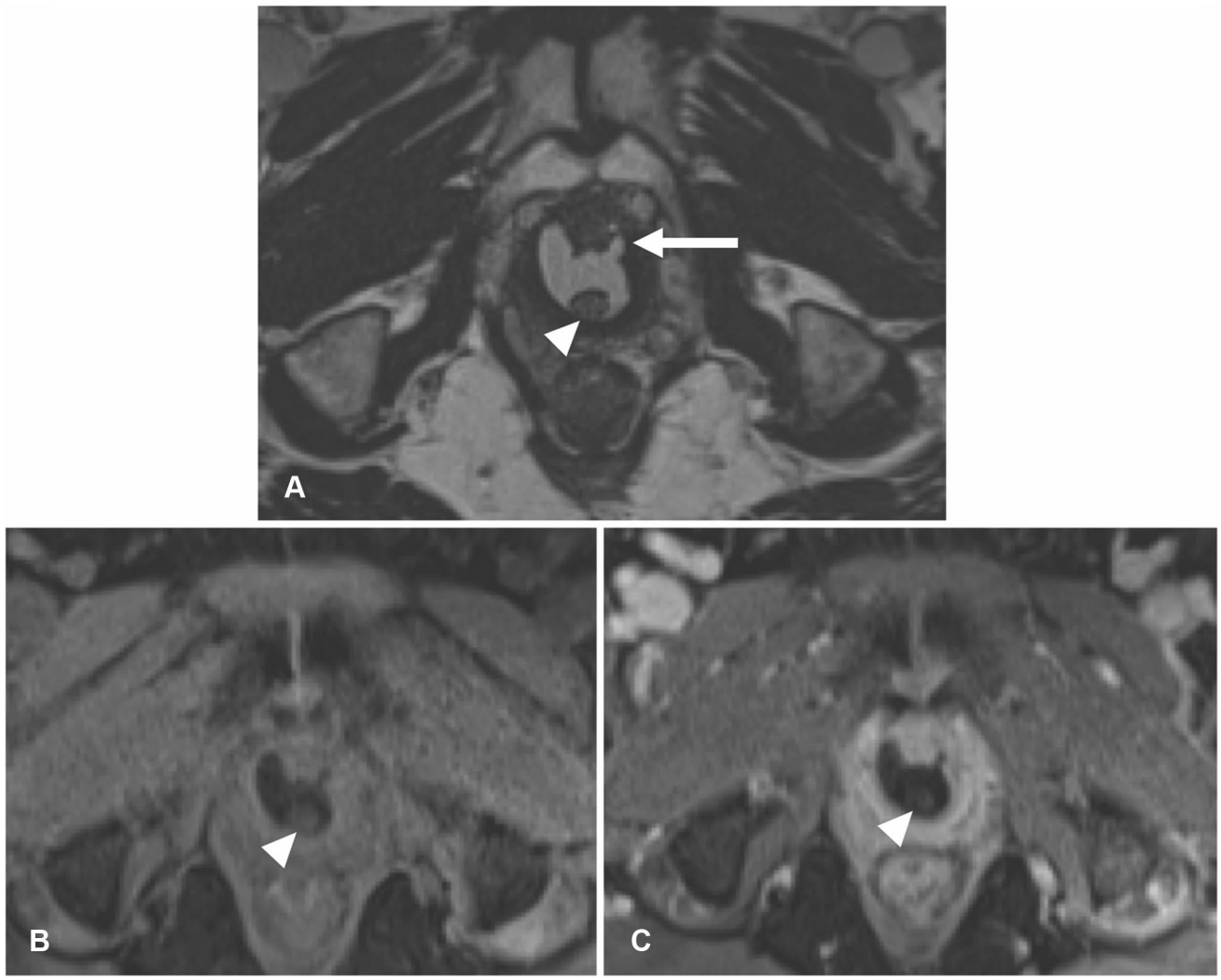

Fig. 3 Urethral diverticulum with a thin neck and stone. **a** Axial T2WI demonstrates a thin neck (arrow) arising from the 1 o'clock position and a hypointense stone (arrowhead). Axial T1-weighted images prior to (**b**) and following contrast (**c**) demonstrate a mildly hyperintense stone with no enhancement (arrowheads)

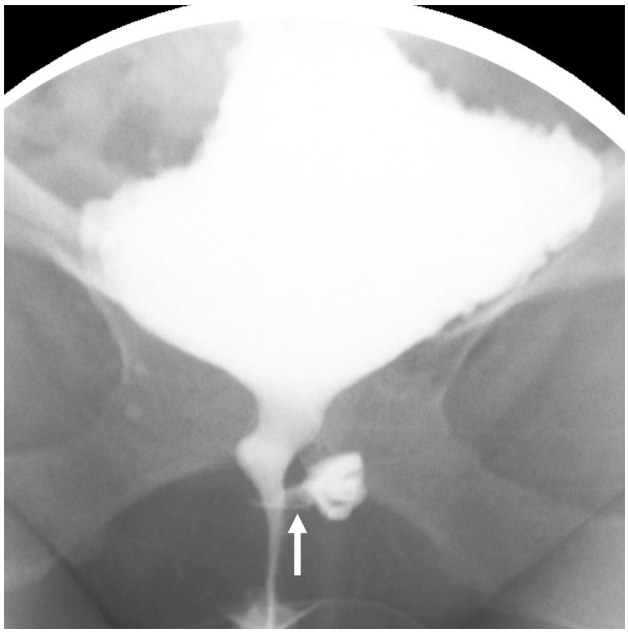

Fig. 4 VCUG after transvaginal diverticulum resection demonstrates a residual diverticulum arising from the 3 o'clock position with a thin neck (arrow). Urethral diverticula frequently recur, particularly if the neck is not fully resected

to prevent urethral injury. When obstructed, Skene gland cysts form. They are lined by stratified squamous epithelium and therefore have a small theoretical risk of squamous cell carcinoma. These lesions are usually hyperintense on T2WI and have variable hyperintensity on T1WI due to protein content. Because of the distal/perineal location, Skene gland cysts and Bartholin gland cysts can be mistaken for each other, however, Skene gland cysts will be *midline*, and the sagittal view will demonstrate a cyst that is located anteriorly *within the plane of the urethra* (Fig. 5a). Infected cysts are treated with antibiotics, and large/symptomatic cysts are treated with surgical fulguration. It is important to distinguish Skene gland cysts from other vaginal cysts (described below), as surgical fulguration of Skene gland cysts can present an increased risk of injury to the urethra.

Bartholin glands, analogous to the male bulbourethral glands, are located on either side of the posterolateral inferior third of the vagina, below the pubic symphysis level, and secrete fluid to lubricate the vagina. Bartholin gland cysts are caused by obstruction of the underlying glands, can be up to 4 cm in size, are typically hyperintense on T2WI, and variable on T1WI depending on internal hemorrhage or protein. These cysts will be *paramedian*, and lie in a *plane posterior to the urethra* (Fig. 5b). Similar to Skene gland cysts, Bartholin cysts are usually incidental and asymptomatic, but may require treatment if large or infected.

Gartner duct cysts are embryologic retention cysts classically located along the anterolateral mid-vagina above the pubococcygeal line. These lesions are hyperintense on T2WI when simple, but can demonstrate varying degrees of hyperintensity on T1WI from hemorrhage or protein. Gartner duct cysts mimic urethral diverticula given their location along the mid-urethra, however, they are centered within the vaginal wall and do not distort or wrap around the urethra (Fig. 5c). These cysts can also be associated with abnormalities of the ipsilateral ureter and kidney, which can be a clue to their diagnosis and pertinent associated findings to report.

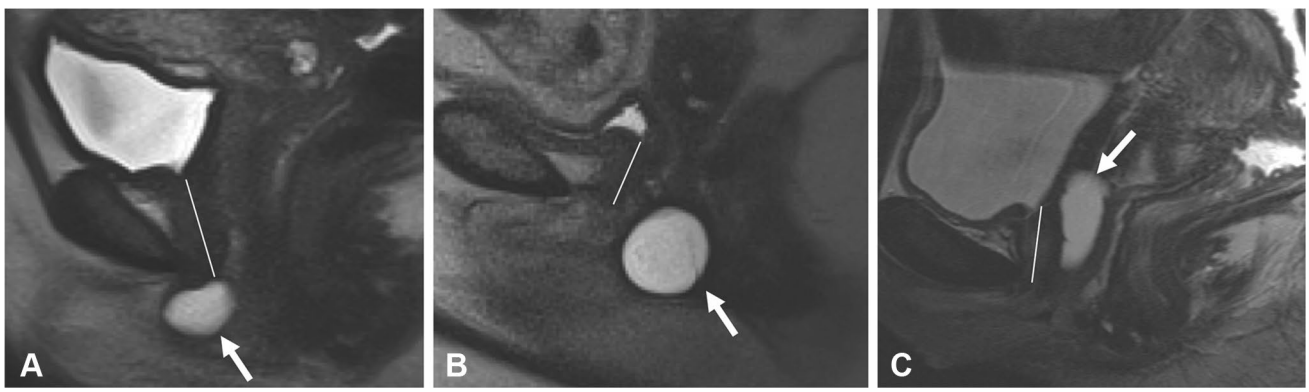

Fig. 5 Urethral/periurethral cysts can be diagnosed based on location. Sagittal T2-weighted images from three different patients reveal a Skene's gland cyst (**a**), Bartholin gland cyst (**b**), and Gartner duct cyst (**c**). **a** The Skene's gland cyst (arrow) is centered on the distal urethra, and located within the plane of the urethra (white line). **b** The Bartholin gland cyst (arrow), arises from the distal vagina/perineum below the pubic symphysis and is posterior to the plane of the urethra (white line). **c** Large Gartner duct cyst arises from the superior and anterior vaginal wall (arrow), posterior to the upper-mid-urethra (thin line)

Benign solid lesions: leiomyoma, endometrioma, hemangioma, and caruncle

Although benign solid lesions of the female urethra are rare, knowledge of their existence can prevent misdiagnosis of a malignant tumor [8]. Leiomyomas are rare benign smooth muscle tumors that arise from the smooth muscle of the proximal posterior urethra [9]. Non-degenerating leiomyomas have similar imaging characteristics to a uterine fibroid, demonstrating well-defined borders, hypointensity on T2WI, and homogeneous contrast enhancement. These lesions may enlarge during pregnancy, suggesting a hormonal dependence [10].

Rarely, endometriomas can implant along the urethra during surgical procedures. As with other endometriomas, T1 hyperintense foci on MRI suggestive of hemorrhage are a strong clue. Infiltrating endometriosis with T2 hypointense bands of fibrosis on MRI are also keys to diagnosis. Hemangiomas can occur at any location in the genitourinary tract and are more commonly found in men, however, can occasionally present in women with hematuria or urethral bleeding. These lesions may be hyperintense on T2WI (similar to liver hemangiomas) and tend to recur [11]. Finally, urethral caruncles are fairly common lesions in postmenopausal patients, presenting as fleshy outgrowths from the posterior urethral meatus and usually definitively diagnosed by physical exam [12].

Urethral malignancy: urothelial carcinoma, squamous cell carcinoma and adenocarcinoma

Primary urethral cancer (PUC) is rare, with an increased incidence in African American women [13, 14]. Risk factors include chronic irritation and infection and the presence of diverticula. Additionally, there is an association with human papilloma virus (HPV) infection, particularly HPV16 [15, 16].

The type of cancer depends on the location along the urethra due to the varying epithelium, with urothelial cancers occurring in the proximal 1/3, squamous cell cancers occurring in the distal 2/3, and adenocarcinoma occurring anywhere along the urethra, owing to distribution of paraurethral glands along the entire urethra. Earlier publications have reported that adenocarcinoma is the least common type of PUC in women and men, however a 2018 study by Aleksic et al. reports that adenocarcinoma is the most common type in women, accounting for up to 46.7% of urethral tumors, likely due to its propensity to develop within a diverticulum [15, 17]. Melanoma can also occur in the female urethra, although rarely.

PUC presentation is variable but often suggestive of stricturing or irritation symptoms. The onset is insidious, and the tumor is locally advanced at the time of diagnosis. Differentiation of the anatomic location of the tumor is important. Those located in the proximal 2/3 of urethra, called 'entire' tumors, drain to pelvic nodes, while those in the distal 1/3 of urethra, called 'anterior' tumors, drain to inguinal nodes. Anterior tumors tend to present earlier and at a less advanced stage.

Direct urethroscopy is the most sensitive test for diagnosis and tissue sampling. Radiologic studies are limited in establishing a diagnosis. VCUG may show an obstructing lesion or filling defect within a urethral diverticulum but fails to show extraluminal tumor extension [3]. MRI has become the staging modality to evaluate for extent of disease, invasion of adjacent organs such as the vagina and bladder, and pelvic adenopathy [3, 8]. For advanced tumors, PET-CT can also be utilized for full-body staging.

Squamous cell and urothelial tumors typically demonstrate low-signal intensity on T1WI, low to intermediate signal on T2WI, and heterogeneous enhancement (Fig. 6). Adenocarcinoma, on the other hand, may have a higher signal on T2WI. Disruption of the normal dark signal on T2WI of the outer muscle layer indicates deep tumor extension (Fig. 7). Tumor within a diverticulum will appear as a filling defect with intermediate to high signal on T2WI and enhancement (Fig. 8).

Because of how rare female urethral cancers are, there is no consensus on standardized treatment options. Superficial tumors are generally curative with surgery. Anterior tumors tend to present at an earlier stage and have a better prognosis. For anterior tumors, ablation or surgery alone, or sometimes radiation alone may be utilized. Entire urethral tumors are typically treated with various multimodality approaches in addition to extensive pelvic surgery [13]. Deeply invasive tumors are rarely cured despite multimodality treatment [18].

Pelvic floor dysfunction: diagnosing cystocele and urethral hypermobility

Weakening of the pelvic floor muscular hammock results in prolapse and dysfunction of pelvic organs, contributing to constipation, pain, and urinary and fecal incontinence. The full range of pelvic floor dysfunction is beyond the scope of this article, however urethral and bladder dysfunction will be discussed.

Stress urinary incontinence (SUI) is defined as the loss of urine with effort, strain, coughing, or sneezing. This disorder affects up to 38% of women over the age of 60, and over 77%

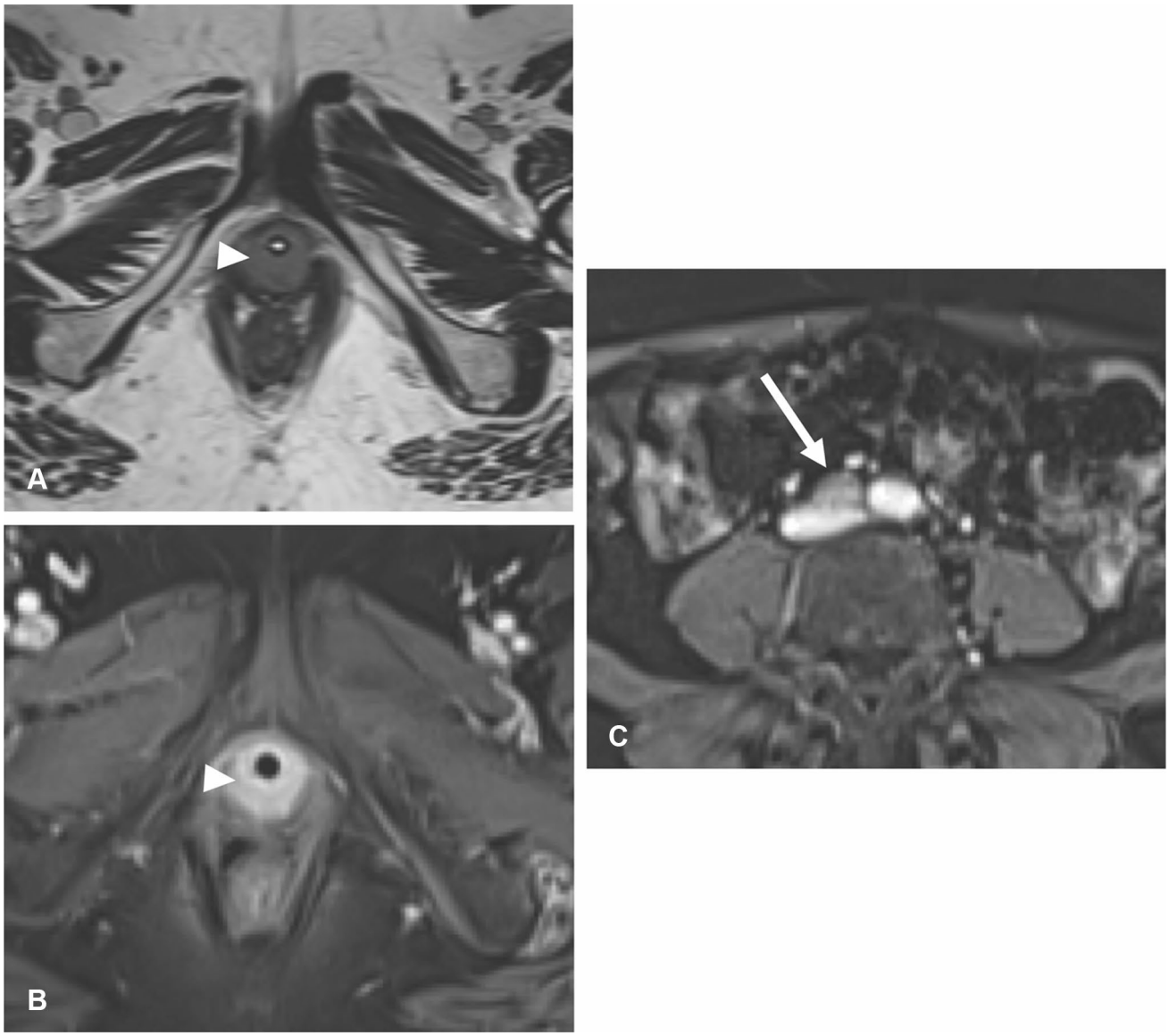

Fig. 6 Urothelial carcinoma. A 65-year-old woman with irritative voiding symptoms. **a** Axial T2WI demonstrates loss of the normal zonal anatomy and intermediate signal tumor (arrowhead)-infiltrating the urethra. **b** Post-contrast T1-weighted image shows diffuse enhancement (arrowhead). **c** Post contrast T1WI higher in the pelvis shows an enlarged aortocaval lymph node (arrow), compatible with nodal metastatic disease. Staging of known urethral malignancy should include images of the pelvis to at least the aortic bifurcation

of women in nursing homes [19, 20]. SUI decreases quality of life and is severe enough to require surgery in 10% of patients [3]. Major risk factors include age, multiparity, vaginal delivery, hysterectomy and obesity. SUI has two main causes: pelvic floor dysfunction (as evidenced by urethral hypermobility which can be diagnosed with dynamic MRI) and intrinsic sphincter deficiency (ISD). Patient with pelvic floor dysfunction are more likely to respond to surgery than those with ISD [21], so distinguishing between the two is critical. Although urogynecologists primarily diagnose SUI by cough stress tests and urodynamic studies, dynamic MRI can add information about anterior compartment dysfunction including the presence of a cystocele and urethral hypermobility, and multi-compartment involvement.

Accepted criteria for a cystocele includes descent of the bladder during Valsalva of more than 1 cm below the pubococcygeal line, a line drawn from the inferior margin of the pubic symphysis to the last joint of the coccyx on a midline sagittal image [21]. A descent of 1–2 cm is considered mild bladder prolapse, 2–4 cm is moderate and >4 cm is severe (Fig. 9). Hypermobility of the urethra is defined a change in the angle of the urethra to the

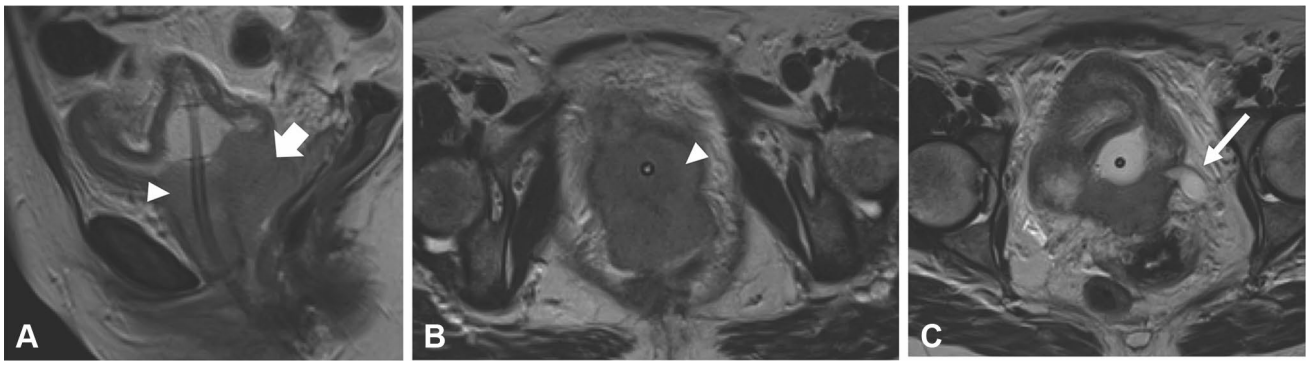

Fig. 7 Extensive squamous cell carcinoma of the urethra invading the vagina and bladder. Sagittal (**a**) and axial (**b**, **c**) T2-weighted images of the pelvis show intermediate signal tumor (arrowheads) invading the vagina (short arrow) and bladder, and causing obstruction of the distal left ureter (long arrow)

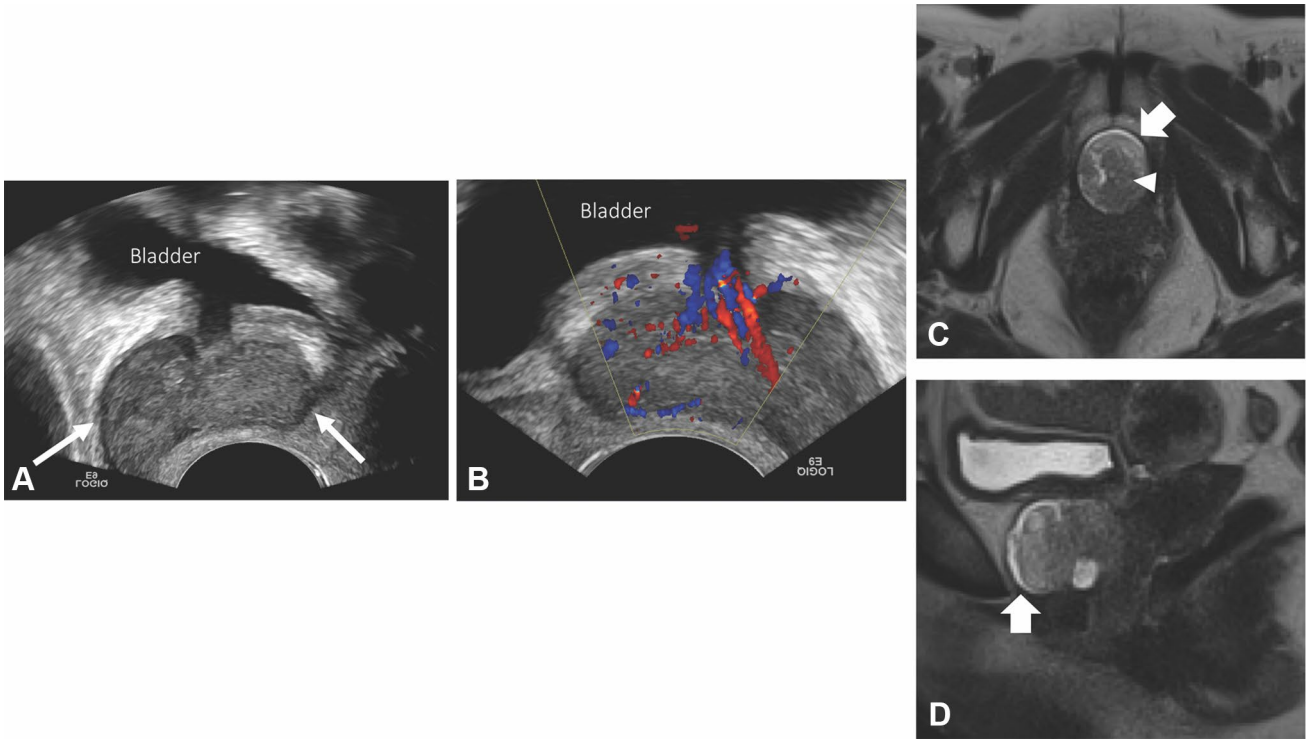

Fig. 8 A 59-years-old woman underwent ultrasound for urinary retention and pelvic pain. **a** Angling the transvaginal probe anteriorly towards the urethra reveals a large mass in the expected location of the urethra (arrows), demonstrating vascular flow on color Doppler ultrasound (**b**). T2-weighted images in the axial (**c**) and sagittal (**d**) plane again show the large tumor with intermediate signal (arrowhead), however, the surrounding fluid (arrows) makes it clear that this tumor arose within a diverticulum. Final pathology revealed adenocarcinoma, the most common type of tumor arising within a urethral diverticulum

vertical plane by greater than 30° between rest and strain (Fig. 10). MRI can also assess supporting structures such as the puborectalis muscle and the intricate network of periurethral ligaments [22]. Macura et al. found that 70% of continent control patients had intact and symmetric periurethral ligaments compared to only 20% of incontinent women [21].

Pelvic floor dysfunction: surgical intervention including sling procedures and injection of bulking agents

SUI is usually treated non-surgically by physical therapy and life-style modification that include wearing pads, avoiding caffeine and overhydration, or by pessaries with

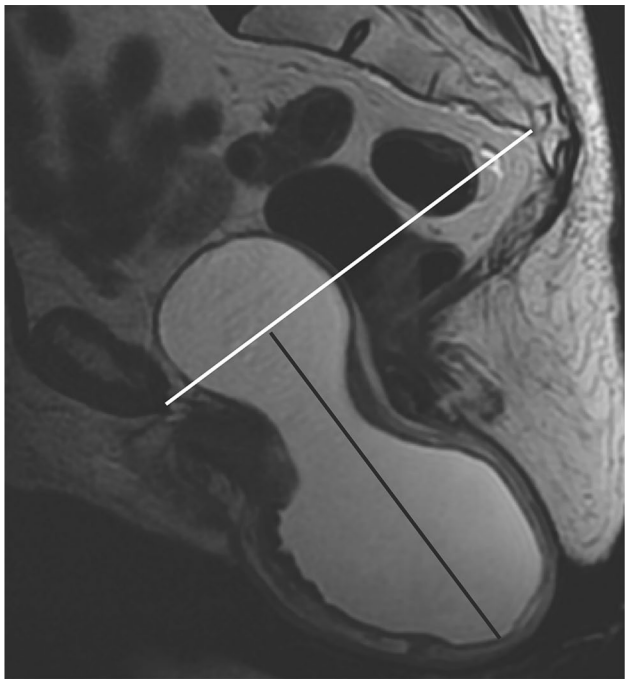

Fig. 9 Severe cystocele. A 73-year-old patient with clinically apparent cystocele presented for pelvic MRI to evaluate the cystocele and for multi-compartment involvement. T2-weighted image shows a severe cystocele extending below the pubococcygeal line (white line) for approximately 8 cm (black line). The uterus has been removed and the rectum does not demonstrate pelvic descent

incontinence knobs that place pressure on the bladder neck. In a smaller subset of patients with debilitating symptoms, primary surgical interventions include retropubic urethropexy and mid-urethral sling procedures. Occasionally, urethral bulking agents are injected.

Burch urethropexy, where the periurethral vaginal tissue is suspended to Cooper's ligament or the fibrocartilage of the pubic symphysis, was the gold standard for many years with a high overall cure rate of 69–89% [19]. However, the less invasive and equally effective midurethral sling or transobturator tape has become the new gold standard since its introduction in 1996 [19]. For this 30-min outpatient procedure, a synthetic mesh is placed through a retropubic or transobturator approach. The sling can be visualized as hypointense bands on T2WI (Fig. 11). Efficacy of the sling can be evaluated by dynamic MRI or dynamic US (Fig. 12). Complications such as mesh erosion and infection occur in less than 5% of patients (Fig. 13), but can be quite debilitating.

Urethral bulking agents are utilized more commonly for intrinsic sphinchter deficiency, or reserved for patients with urethral hypermobility who have failed surgery. They are generally less efficacious than slings with cure rates of approximately 25–37% and may require repeat injections [22]. They can be injected in the office under local anesthesia, typically into the submucosal layer to increase mucosal coaptation [23]. The several types of agents demonstrate different ultrasound signal, CT density and MRI signal

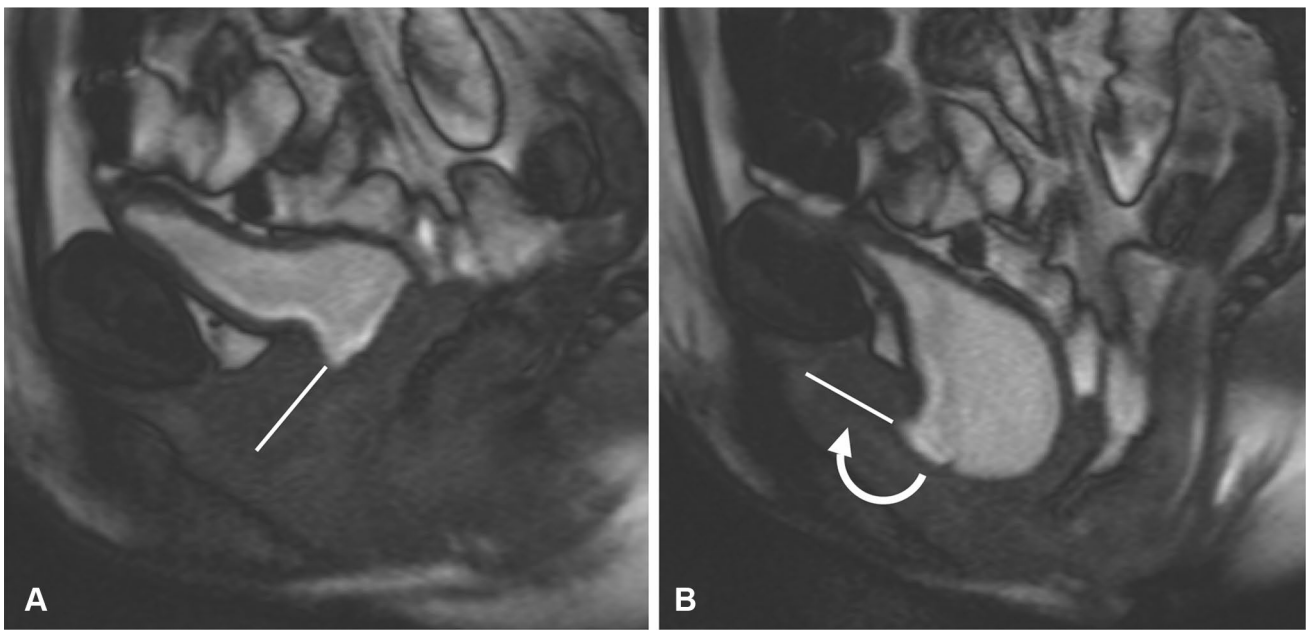

Fig. 10 Moderate-severe cystocele with urethral hypermobility. Sagittal T2-weighted images at rest (**a**) and during Valsalva (**b**) demonstrates descent of the bladder and hypermobility of the urethra (white line), rotating anteriorly more than 30 degrees (curved arrow)

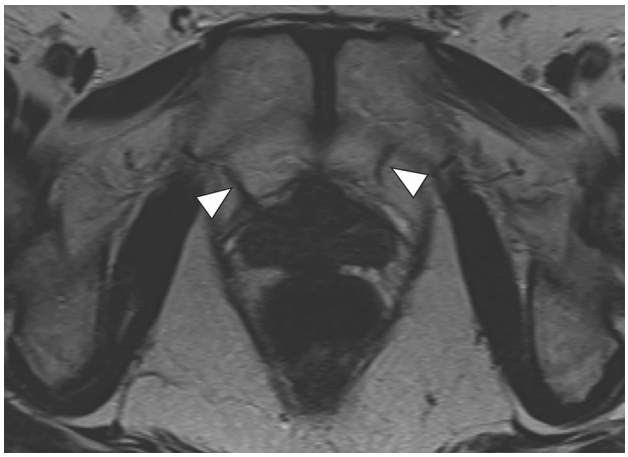

Fig. 11 Normal appearance of a midurethral sling. Axial T2-weighted image demonstrates thin hypointense bands extending from the urethra to the pubic bone (arrowheads), compatible with a synthetic sling

intensity (Fig. 14). For example, carbon-coated microbeads are generally hyperdense on CT, while collagen is closer to water density [24]. Both types of injectable material demonstrate low signal on T2WI, which allows them to be distinguished from fluid-filled urethral diverticula. The ultrasound signal of these lesions varies from hypoechoic to hyperechoic, with the latter mimicking a bladder stone unless a history of bulking procedure is known [25]. Importantly, the lesion should demonstrate no internal vascularity—any color Doppler signal within the lesion should raise concern for a urethral malignancy.

Conclusion

Female urethral pathology can be challenging to diagnose due to non-specific clinical symptoms and inability to visualize pathology on physical exam. High-resolution MRI with a dedicated female urethra protocol has become a powerful tool in the diagnosis of urethral lesions and staging of malignancy. Diverticula, the most common lesion of the female urethra, can be characterized for pre-surgical planning and distinguished from other periurethral cysts such as Skene gland, Batholin gland and Gartner duct cysts. Solid masses of the urethra, particularly those that obliterate the normal zonal anatomy and infiltrate into periurethral tissues, are highly concerning for malignancy and have a poor prognosis, therefore early diagnosis is key. Stress urinary incontinence is a common and debilitating condition, and dynamic MRI, fluoroscopy or ultrasound can critically evaluate for pelvic floor prolapse as well as effectiveness of slings and injections. Using optimal technique and a combination of MRI and dynamic imaging, a comprehensive evaluation of the female urethra can be achieved.

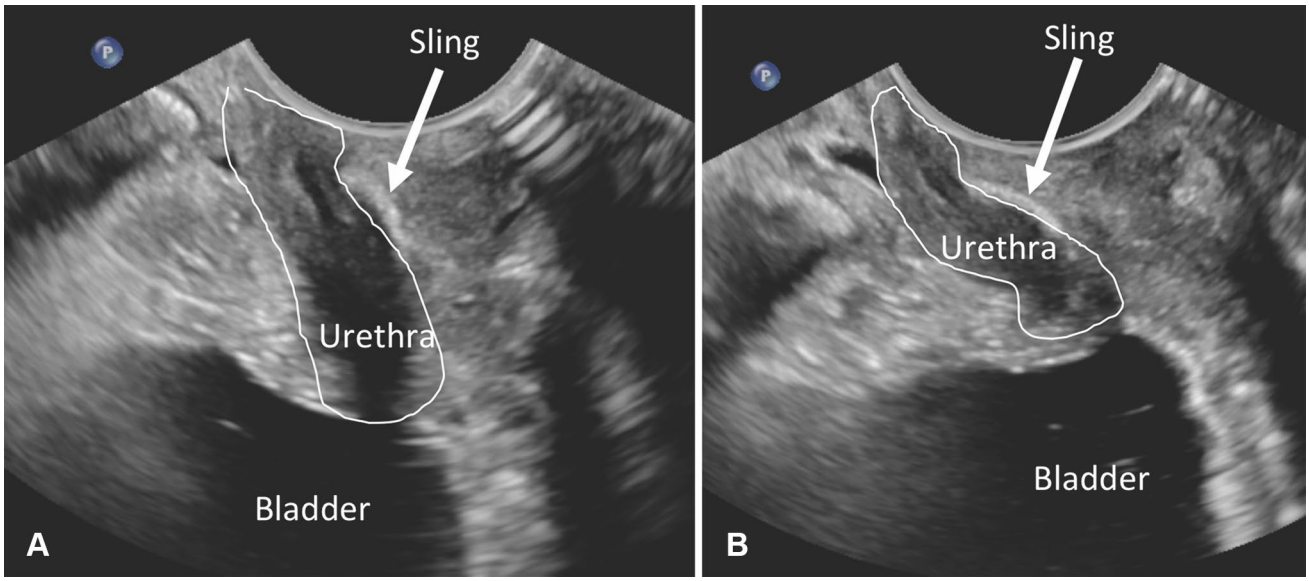

Fig. 12 Evaluation of a midurethral sling by dynamic ultrasound. Transvaginal ultrasound of the urethra at rest and during valsalva. **a** At rest, the urethra (outlined) and posterior aspect of the sling (arrow) are in expected position. **b** During Valsalva, there is minimal mobility of the urethra (outlined) suggesting that the sling is appropriately functioning. Case courtesy of Dr. Gaurav Khatri, University of Texas Southwestern

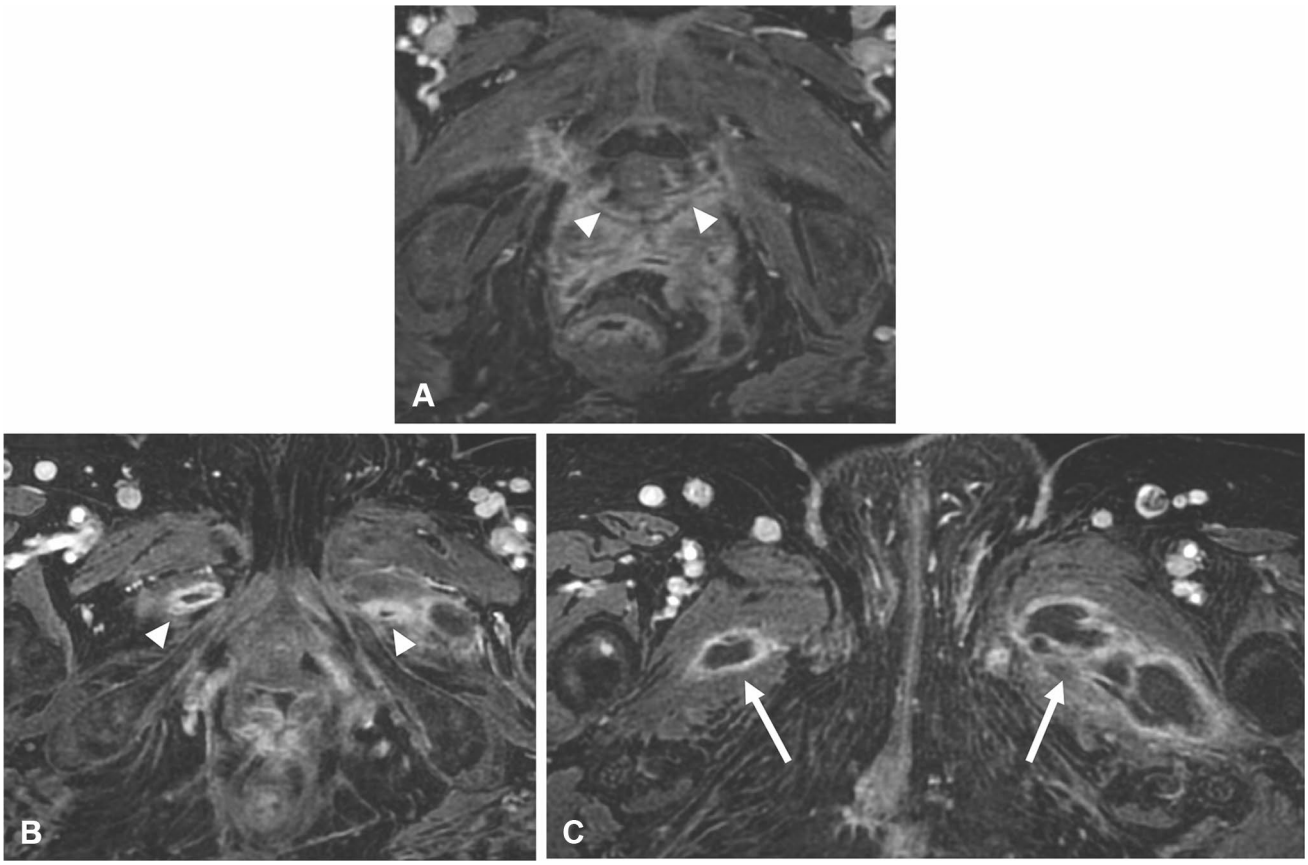

Fig. 13 Urethral sling infection. A 70-year-old female with fevers, pain, and difficulty walking 3 weeks after suburethral sling procedure with transobturator approach. Post-contrast T1-weighted images (**a**–**c**) at three different levels demonstrate avid enhancement and inflammation along the sling (arrowheads), and bilateral adductor muscle abscesses coursing inferiorly from the sling insertion sites (arrows). The sling and graft were removed and multiple abscess drainages were performed

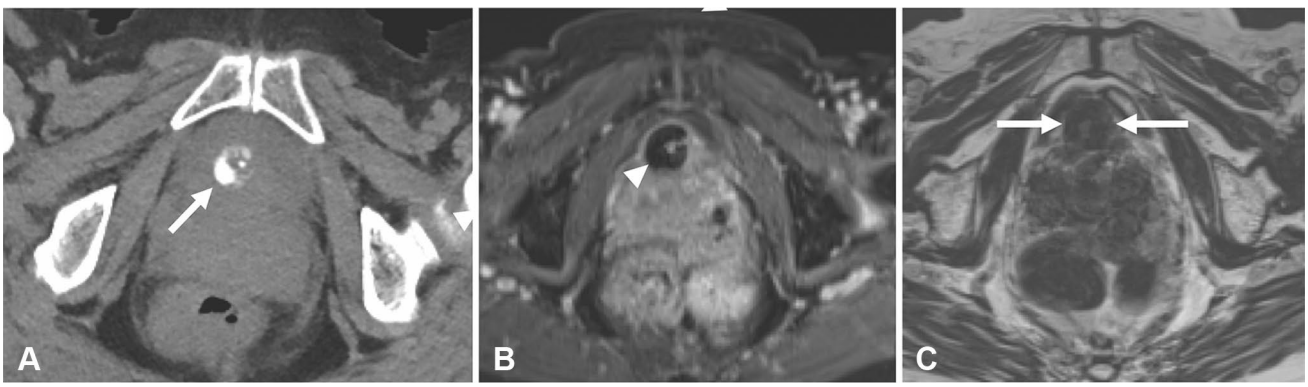

Fig. 14 Periurethral carbon-coated bead injection on CT and MRI. 62-years-old female who was a poor surgical candidate underwent collagen injection into the submucosal layer of the urethra. **a** CT demonstrates dense material wrapping around the urethra (arrow), more compatible with carbon injection than collagen. **b** Axial T1-weighted post-contrast image demonstrates a non-enhancing lesion wrapping around the urethra (arrowhead), mimicking a urethral diverticulum. **c** Axial T2-weighted image demonstrates markedly hypointense signal (arrows), more compatible with injected bulking agent than a diverticulum

References

1. Jung J, Ahn HK, Huh Y (2012) Clinical and Functional Anatomy of the Urethral Sphincter. Int Neurourol J 16:102-106
2. Itani M, Keiler A, Menias CO, Dighe MK, Surabhi V, Prasad SR, O'Malley R, Gangadhar K, Lalwani N (2016) MRI of the female urethra and periurethral pathologies. Int Urogyn J 27:195-204
3. Chaudhari VV, Patel MK, Douek M, Raman SS (2010) MR Imaging and US of Female Urethral and Periurethral Disease. RadioGraphics 30:1857-1874
4. Bennett GL, Hecht EM, Tanpitukpongse TP, Babb JS, Taouli B, Wong S, Rosenblum N, Kanofsky JA, Lee VS (2009) MRI of the urethra in women with lower urinary tract symptoms: spectrum of findings at static and dynamic imaging. American Journal of Roentgenology 193:1708-1715
5. Prasad SR, Menias CO, Narra VR, Middleton WD, Mukundan G, Samadi N, Heiken JP, Siegel CL (2005) Cross-sectional Imaging of the Female Urethra: Technique and Results. RadioGraphics 25:749-761
6. Kawashima A, Sandler CM, Wasserman NF, LeRoy AJ, King BF, Goldman SM (2004) Imaging of Urethral Disease: A Pictorial Review. RadioGraphics 24:S195-S216
7. Patel AK, Chapple CR (2006) Female urethral diverticula. Curr Opin Urol 16:248–254
8. Del Gaizo A, Silva AC, Lam-Himlin DM, Allen BC, Leyendecker J, Kawashima A (2013) Magnetic resonance imaging of solid urethral and peri-urethral lesions. Insights Imaging 4:461-9
9. Kwang NB, Naidu A, Yahaya A, Shan LP (2016) Urethral Leiomyoma: A Rare Clinical Entity. Case Rep Surg 2016:6037104
10. de Lima Jr MM, Sampaio CB, Ticianeli JG, de Lima MM, Granja F (2014) Leiomyoma - a rare benign tumor of the female urethra: a case report. J Med Case Rep 8:366
11. Kanthikar SN, Nikumbh DB, Dravid NV, Rokade CM (2015) Female urethral cavernous hemangioma - An unusual case of hematuria. A rare case report. Clin Cancer Investig J 4: 462-464
12. Tomita H, Takeyama N, Hayashi T, Tanihuji S, Yamamoto K, Sasaki H, Ohike N, Nakajima Y, Hashimoto T (2017) Magnetic Resonance Imaging of a Urethral Caruncle and the Pathologic Correlation: A Report of 3 Cases. JCAT 41: 962-964
13. Dayyani F, Hoffman K, Eifel P, Guo C, Vikram R, Pagliaro LC, et al (2014) Management of advanced primary urethral carcinomas. BJU Int 114:25-31
14. Swartz MA, Porter MP, Lin DW, Weiss NS (2006) Incidence of primary urethral carcinoma in the United States. Urology 68:1164–1168
15. Aleksic I, Rais-Bahrami S, Daugherty M, Agarwal PK, Vourganti S, Bratslavsky G (2018) Primary urethral carcinoma: A Surveillance, Epidemiology, and End Results data analysis identifying predictors of cancer-specific survival. Urol Ann 10:170-174
16. Wiener JS, Walther PJ (1994) A high association of oncogenic human papillomaviruses with carcinomas of the female urethra: polymerase chain reaction-based analysis of multiple histological types. J Urol 151:49-53
17. Chou CP, Levenson RB, Elsayes KM, Lin Y.H, Fu TY, Chiu YS, Huang JS, Pan HB (2008) Imaging of Female Urethral Diverticulum: An Update. RadioGraphics 28:1917-1930
18. PDQ® Adult Treatment Editorial Board. PDQ Urethral Cancer Treatment. National Cancer Institute. https://www.cancer.gov/types/urethral/hp/urethral-treatment-pdq. Accessed 24 March 2019
19. Lucacz ES, Santiago-Lastra Y, Albo ME (2017) Urinary Incontinence in Women: A Review. *JAMA* 318:1592–1604
20. Thom DH, Brown JS (1998) Reproductive and Hormonal Risk Factors for Urinary Incontinence in Later Life: A Review of the Clinical and Epidemiologic Literature. J Am Geriatr Soc 46:1411-1417
21. Macura KJ, Thompson RE, Bluemke DA, Genadry R (2015) Magnetic resonance imaging in assessment of stress urinary incontinence in women: Parameters differentiating urethral hypermobility and intrinsic sphincter deficiency. World J Radiol 7: 394-404
22. El Sayed RF, Morsy MM, El Mashed SM, Abdel-Azim MS (2007) Anatomy of the Urethral Supporting Ligaments Defined by Dissection, Histology, and MRI of Female Cadavers and MRI of Healthy Nulliparious Women. AJR Am J Roentgenol 189:1145-1157
23. Mamut A, Carlson K (2017) Periurethral bulking agents for female stress urinary incontinence in Canada. Can Urol Assoc J 11:S152-154
24. Bridges MD, Petrou SP, Lightner DJ (2005) Urethral Bulking Agents: Imaging Review. AJR Am J Roentgenol 185: 257-264
25. Denson L, Shobeiri SA (2013) Imaging of Urethral Bulking Agents: A Sonographer's Perspective. Journal of Diagnostic Medical Sonography 29:255-259